WRR Technical Note
November 2001

Flow Channeling and Analysis of Tracer Tests in Heterogeneous Porous Media

Luis Moreno[1] and Chin-Fu Tsang[2]

1 Department of Chemical Engineering and Technology
Royal Institute of Technology, Stockholm, Sweden
E-mail: lm@ket.kth.se

2 Earth Sciences Division
Ernest Orlando Lawrence Berkeley National Laboratory
Berkeley, USA

ABSTRACT

Flow and solute transport through porous medium with strongly varying hydraulic conductivity are studied by numerical simulations. The heterogeneity of the porous medium is defined by σ and λ', which are, respectively, the standard deviation of natural log of permeability values and its correlation range λ divided by transport distance L. The development of flow channeling as a function of these two parameters is demonstrated. The results show that for large heterogeneities, the flow is highly channelized and solute is transported through a few fast paths, and the corresponding breakthrough curves show a high peak at very early times, much shorter than the mean residence time.

This effect was studied for a converging radial flow, to simulate tracer tests in a fracture zone or contact-thickness aquifer. It is shown that $\sigma^2\lambda'$ is an appropriate parameter to characterize the tracer dispersion and breakthrough curves. These results are used to study tracer breakthrough data from field experiments performed with nonsorbing tracers. A new procedure is proposed to analyze the results. From the moments of the residence-time distribution represented by the breakthrough curves, the heterogeneity of the porous medium, as characterized by $\sigma^2\lambda'$ and the mean residence time t_o, may be determined.

Introduction

Solute dispersion in a porous medium is caused mainly by the variability of the fluid velocities in it, which in turn are caused by the variation in the medium's hydraulic conductivity. Because of dispersion, a fraction of contaminants dissolved in the fluid is transported with velocities larger than the average velocity of the fluid. In practical problems involving transport of radioactive or toxic wastes, the early arrival of contaminants may be of vital importance. Generally, heterogeneous porous media can be characterized by statistical distributions of hydraulic conductivity, which may, e.g., for a lognormal distribution, be described by its geometric mean, the standard deviation, and its correlation structure (if it exists).

In an earlier paper, Moreno and Tsang (1994) studied fluid flow and solute transport in a three-dimensional porous medium with strongly variable hydraulic properties. Strong channeling effects were observed in the porous medium with large heterogeneity, as measured by σ the standard deviation of the natural log permeability values. Flow channeling is also influenced by the way that heterogeneities are distributed in the porous media, as described by the correlation length λ.

In this paper, the effects of the correlation structure and the variance in hydraulic conductivity are studied on flow and transport in a porous medium. From the tracer breakthrough curves the moments for the residence times are calculated, and a spreading measure is obtained. A procedure is then proposed to analyze the results of experimental tracer tests performed with nonsorbing tracers. The objective of the new procedure is to obtain an estimate of the heterogeneity of the porous medium.

Calculation of tracer transport in heterogeneous media

Solute transport through porous media is affected by the variability of the medium permeability and the way this variability is distributed in the system. The highest fluid rates are found along the least-resistive pathways and vice versa. In this paper, these effects are studied numerically.

The porous medium block in the model is divided into cubic cells or grid elements of dimension ΔL_x, ΔL_y, ΔL_z, where the three lengths are equal. The number of nodes used is $N_x \times N_y \times N_z$. The hydraulic conductivity is assigned to each element assuming that the hydraulic conductivity is log-normally distributed and correlated in space. An exponential covariance function is used. The conductivity field is generated using a geostatistical software library (Deutsch and Journel, 1998). For each realization, a conductivity field with a given correlation structure is generated. From this field, grids with different standard deviations are generated. Standard deviation is varied over a wide interval, from 0.5 to 6.0 (in natural log). Hydraulic conductivities are generated with ratios of correlation range to transport length in the interval 0.1-0.4.

Flow calculations are based on steady flow conditions and follow the procedure used by Moreno and Tsang (1994). For given boundary conditions, the hydraulic heads in the nodes are calculated. Two cases are studied. In the first case, a cubic block of heterogeneous porous medium is assumed with $N_x = 40$; $N_y = 40$ and $N_z = 40$. A step in hydraulic head is applied to the top and bottom faces of the cube and the four side faces are closed to flow. In the second case, a radially converging regional flow is simulated by extraction at one corner of the xy-plane, with $N_x = 250$, $N_y = 250$ and $N_z = 1$. No-flow conditions are assumed for all planes, and the fluid is introduced along a circle at a given distance from the extraction point. The hydraulic conductivities of locations beyond the circle were set to be very large in order to simulate the cylindrical regional flow. Once the flow is calculated, the fluid velocity may be calculated, assuming the flow porosity is known. In this paper, for simplicity, flow porosity is assumed to be uniform.

Solute transport through the porous medium is simulated by a particle-tracking technique. Four thousand particles are introduced into the fluid at specified inlet nodes. The number of particles introduced in each inlet node is proportional to the flow in that node and randomly distributed on its surface. The particle tracking is carried out calculating the velocity v of the particle in its actual location and then move the particle a small distance $v \cdot \Delta t$, with the time step set small enough to get reliable results. Velocity is calculated using a three-dimensional interpolation scheme by linear interpolation among the velocity vectors from the node where the particle is

located to all the adjacent nodes. In these calculations, no local dispersion within each path is considered. The particles are collected at outlet nodes and the travel time for each particle is recorded.

The emergence of channeling

Flow and solute transport in a regional parallel flow system in an isotropic medium are calculated for several realizations. The hydraulic head at the inlet is set equal to H_H and the hydraulic head at outlet is set to be H_L, corresponding to high and low hydraulic head respectively.

If solute is injected as a pulse in the upstream face of the cubic heterogeneous porous block, with $N_x = 40$, $N_y = 40$ and $N_z = 40$, the solute concentration at the outlet will be dispersed as a result of the different velocities in various flow paths traversed by the solute from the inlet to the outlet face. In addition to this velocity variation due to permeability heterogeneity, there is also a smaller scale variation due to hydrodynamic dispersion within the pores. This would be added to the "macro-dispersion" caused by the different flow paths. However, the hydrodynamic dispersion is not included in the particle tracking technique used in the present simulations since we are interested to study only the macro-dispersion caused by the different velocities in the various flow paths. It can be straightforwardly added if needed.

The fluid flow seeks the less resistive pathways, therefore the flow through a heterogeneous medium takes place in channels. These channels are not physical entities, meaning that if the direction of the hydraulic gradient is changed the locations of the channels are also changed (Tsang and Tsang, 1989). The emergence of channeling as a function of the degree of the heterogeneity is shown Figure 1 for one realization. A value of 0.2 is chosen for the λ', the ratio of the correlation range λ to transport distance L; i.e., $\lambda' = \lambda/L$. For small standard deviation of permeability, $\sigma = 0.5$ in natural log, flow is essentially vertical with little contrast between fast and slow flows. However, As σ is increased to 2.0 and 6.0, flow becomes highly channelized, with exit flow on the lower boundary concentrated at a few discrete locations.

Flow channeling also depends on the spatial correlation range as a fraction of flow distance λ'. Figure 2 shows the results for one realization for a standard deviation in hydraulic conductivity distribution of 2.0. For small correlation range, λ' of 0.1, channeling occurs, but the channels are closely spaced, and there are many of them over the flow domain. The channeling effect is "averaged out." especially if hydrodynamic dispersion is present. However, for larger values of correlation ranges (e.g., λ' of 0.2 and 0.4), it is found that flow channeling is important and is not very sensitive to the exact λ' value.

Figure 3 shows breakthrough curves for different standard deviations in conductivity distribution for two different ratios of between correlation range to travel distance. For correlation ranges of 0.40 of the flow domain, breakthrough curves show a clear peak at unit time for small heterogeneity. When the heterogeneity increases (larger σ), the peak is wider and moves in the direction of shorter travel times. If the heterogeneities are extremely large ($\sigma = 4$ or 6), the curves present a clear peak, which occurs for very short travel times. This means that for large heterogeneities, a fraction of the solute is transported through a channel with a large flow. Large contrasts between velocities (in between channels) are observed.

When a small correlation length (correlation range of 0.10 of the flow domain) is used, a thin peak at unit time is obtained for porous media with small standard deviation in conductivity distribution ($\sigma = 0.5$). If the degree of the heterogeneities is increased, the peak is wider and moves slightly to shorter times. No clear peak is observed for extremely large heterogeneities ($\sigma = 4$ or 6).

Tracer breakthrough curves and heterogeneity

From the well-known one-dimensional advection-dispersion equation, a dimensionless Peclet number, Pe, can be defined that relates the dispersion with the advection and is defined as

$$\mathrm{Pe} = \frac{\mathrm{L}}{\alpha} \tag{1}$$

where L the apparent (macroscopic) travel distance and α the dispersivity. Robinson (1984) calculated the dispersion as a function of the first and second moments of the particle travel time, $<t>$ and $<t^2>$, or alternatively as a function of the moments of the inverse travel time, $<t^{-1}>$ and $<t^{-2}>$. In this paper, let us use Robinson's expression for Pe based on the moments of the inverse travel time, so that the Pe is not dominated by the long tail of the tracer breakthrough curve at large times,

$$\mathrm{Pe} = \frac{\left(3r^2 - 2\right)^{0.5} - 4}{\left(3r^2 - 2\right)^{0.5} - 1} \qquad \text{where } r = \frac{< t^{-2} >}{< t^{-1} >^2} \tag{2}$$

Further, it is found (Gelhar and Axness, 1983) that for an isotropic porous medium, α increases directly with the variance of log hydraulic conductivity and the correlation length

$$\alpha = \frac{\sigma^2 \lambda}{\gamma^2} \tag{3}$$

where σ^2 is the variance of the log hydraulic conductivity and λ is the correlation scale. The parameter γ is a flow factor defined as 1 by Neuman et al. (1987) and as $1+\sigma^2/6$ by Gelhar and Axness (1983). For our present discussion, let us follow Neuman et al. (1987) to take $\gamma = 1$.

The set of Equations (1) to (3) represents a direct linear relationship between 1/Pe and $\sigma^2\lambda'$, which is valid for 1D advective-dispersive transport in a medium with moderate values of $\sigma^2\lambda'$.

Now, let us re-plot two pairs of breakthrough curves from Figure 3 having the same $\sigma^2\lambda'$. The first pair includes one curve with $\lambda' = 0.4$ and $\sigma = 2$ and another curve with $\lambda' = 0.1$ and $\sigma = 4$, so that both have the same $\sigma^2\lambda'$ of 1.6. The breakthrough curves are shown in Figure 4a, and they coincide with each other very well. Figure 4b shows the same situation for another pair of breakthrough curves with $\sigma^2\lambda' = 0.4$, where very good agreement is also obtained. Two additional curves are also selected for $\sigma^2\lambda' = 0.1$, and they are also found to be in good agreement with each other. These numerical

results indicate that the use of $\sigma^2\lambda'$ for characterizing breakthrough curves is an adequate approach over the range of σ and λ' values used.

For tracer breakthrough experiments in a fracture zone, a 2D flow field is assumed. In this case we calculate heterogeneous flow in a 2D domain with $N_x = 250$, $N_y = 250$ and $N_z = 1$. The numerically generated tracer breakthrough curves was evaluated using Equation (2) to obtain an apparent 1/Pe number for each curve, and then this is plotted against $\sigma^2\lambda'$ from values used to generate them. In this context, 1/Pe is a measure of tracer dispersion and the plot of 1/Pe against $\sigma^2\lambda'$ is an empirical relationship obtained from simulation of flow and transport in strongly heterogeneous media.

Figure 5 (circles / dashed lines) shows the inverse of the apparent Pe obtained by this method plotted as a function of the product $\sigma^2\lambda'$. A linear relationship exists for most of the interval, with deviations observed for the very large values of $\sigma^2\lambda'$. It is significant that the numerical results still display a linear relationship up to $\sigma^2\lambda' = 10$, which corresponds to quite a large value of σ, since λ' ranges between 0.1 and 0.4.

The results assuming 100% recovery of the injected particles (circles / dashed lines in Figure 5) are not useful from the practical point of view, since it is almost impossible in actual field tests to recover 100 % of the injected tracer. Tracer tests with non-sorbing species carried out over short distances are usually stopped when 80-90 % of the injected tracer is recovered. For tests performed over large distances the recovery of the tracer is usually much less. For this reason, we explore the possibility to determine the apparent 1/Pe using a smaller fraction of the tracer. Consider the case when the peak of the breakthrough curve occurs before 50% of the injected tracer is recovered. Then we calculate the spreading (1/Pe) for data up to 50% recovery. The results (Figure 5) show a good correlation with $\sigma^2\lambda'$ also for this case.

The same approach can be used in the determination of the mean residence time. In order to determine the actual mean residence time, all the injected tracer needs to be recovered. For a porous medium with large heterogeneities, there is a large difference between the actual mean residence time and the time when 50% of the tracer is recovered. However, the time required to recover 50 % of the tracer can be correlated

with the mean residence time. The ratio is calculated numerically as a function of $\sigma^2\lambda'$ and is shown in Figure 6, which can be used to estimate the mean residence time.

Analysis of experimental tracer tests

The procedure described above was applied to three tracer tests with nonsorbing tracers (Amino G, iodide, and uranine) performed at Finnsjön by Andersson et al (1989). The tracers were injected using packers through three boreholes (labeled KF111, KF106 and BF101, respectively) into a horizontal fracture zone. Once the tracers were injected, water was produced from an open borehole (labeled BF102) intersecting the fracture zone located at a distance of 155–189 meters from the injection boreholes. The three injection boreholes are situated in three directions from the production borehole, south, north and east respectively. The recovery ranged from 67 to 81% of the injected mass. Data for the tracer tests are shown in Table 1, and the breakthrough curves are shown in Figure 7.

The spreading of the tracer from each of the tracer injection boreholes at the pumping location was calculated using Equation (2) for 50% of the tracer recovered in the experiments. From the spreading of the tracers (and using Figure 5), the value of the product $\sigma^2\lambda'$ was determined. Mean residence time was obtained by using the arrival time for 50% of the injected tracer and reading off from Figure 6. These results are shown in Table 1.

Table 1. Analysis of the tracer tests in Finnsjön (Andersson et al, 1989)

	Amino G	Iodide	Uranine
Experimental data			
Injection borehole	KF111	KF106	BF101
Direction from Pumping Well (BF102)	S	N	E
Travel distance, m	155	189	168
Recovery, %	71	81	67
From breakthrough curves			
Apparent 1/Peclet (Equation (2))	0.30	0.34	0.16
$\sigma^2\lambda'$ (Figure 5)	9.0	11	6.5
T_{50}, hrs (Data)	15	34	64
Mean residence time, hrs (Figure 6)	31	85	123

Note that Figures 5 and 6 assume tracers reaching the production well sample the whole heterogeneity field. Thus they represent an ensemble average of the tracer release through one injection well. In a tracer test, the result represents a particular realization in which tracer is release at one injection well. To check the results obtained using different values of $\sigma^2\lambda'$, numerical tracer breakthrough curves were calculated for a few realizations using the values of $\sigma^2\lambda'$ obtained above (Table 1). We know only the value of the product $\sigma^2\lambda'$, not the values of σ and λ'. Let us assume that the value of λ' is 0.4 and then proceed to calculate σ and generate multiple realizations of heterogeneous fields for breakthrough curves calculations. The breakthrough curves are shown in Figure 7 together with the experimental breakthrough curves. They bracket the experimental results quite well. Further study along this line, to evaluate range of applicability, is underway.

Conclusions

Flow and solute transport through porous media with strongly varying hydraulic conductivity was studied by numerical simulations. It was found that flow channeling develops as the medium becomes more heterogeneous, as measured by increasing values of σ and λ'. For low standard deviation σ, the tracer breakthrough curves have a clear peak at a relative residence time of 1.0. When σ is increased, the peak is wider and moves toward shorter times. At a very large degree of heterogeneity, the breakthrough curves show a clear peak at very short times. This effect is less for a medium with a smaller correlation length. Numerical results also show $\sigma^2\lambda'$ to be a good parameter characterizing the breakthrough curves up to $\sigma = 6$.

Determination of heterogeneity as measured by $\sigma^2\lambda'$ and tracer mean residence time in a porous medium with strongly varying conductivity may be carried out by tracer tests in which only a fraction of the injected tracer (greater than 50%) is recovered. The heterogeneity of the porous medium in terms of $\sigma^2\lambda'$ is determined using Equation (2) and Figure 5, and the residence time may be determined from the time to recover 50% of the tracer, using the plot in Figure 6. This procedure attempts to relate the tracer breakthrough curves directly with the heterogeneity characteristics of the medium. The proposed method is based on assumption that the heterogeneous

medium can be described by the two parameters σ and λ and that its permeability distribution is lognormal. Further no hydraulic dispersion is present. Other studies are underway to explore the feasibility of this approach.

Acknowledgements

We appreciate the careful review and comments of the Dr Christine Doughty of the Lawrence Berkeley National Laboratory. The first author's work was supported by the Swedish Nuclear Fuel and Waste Management Company (SKB). The second author's work was supported by the Japanese Nuclear Cycle Institute (JNC) under an Annex to a Cooperative Research Agreement between JNC and the United States Department of Energy (DOE) on radioactive waste management, coordinated by DOE's Office of Environmental Management, Office of Science and Technology (EM 50), through Contract Number DE-AC03-765F00098.

References

Andersson, J.E., L. Ekman, E. Gustafsson, R. Nordqvist, and S. Tyrén, Hydraulic interference tests and tracer tests within the Brändan zone, Finnsjön study site, Swedish Nuclear Fuel and Waste Management Co., SKB Technical Report TR-89-12, Stockholm, 1989.

Deutsch, C.V., and A.G. Journel, GSLIB, Geostatistical Software Library and User's Guide, Oxford University Press, 2nd ed., New York, 1998.

Gelhar, L.W. and C.L. Axness, Three-dimensional stochastic analysis of macrodispersion in aquifers, Water Resourc. Res., 19(1), 161–180, 1983.

Moreno L. and C.F. Tsang, Flow channeling in strongly heterogeneous porous media. A numerical study, Water Resourc. Res., 30(5), 1421–1430, 1994.

Neuman, S.P., C.L. Winter, and C.M. Newman, Stochastic theory of field-scale dispersion in anisotropic porous media, Water Resourc. Res., 23(3), 453–466, 1987.

Robinson P.C., Connectivity, flow and and transport in network models of fractured media, Ph. D. Thesis, St. Catherine's College, Oxford University, Ref TP 1072, May 1984.

Tsang Y.W. and C.F. Tsang, Flow channeling in a single fracture as a two-dimensional strongly heterogeneous permeable medium, Water Resourc. Res., 25(9), 2076-2080, 1989.

CAPTIONS OF FIGURES

Figure 1. Emergence of channels for different standard deviation in hydraulic conductivity. A value of 0.20 is used for the integral range.

Figure 2. Emergence of channels for integral range. A value of 2.0 is used for the standard deviation of the conductivity distribution.

Figure 3 Breakthrough curves from a 3-D porous medium. For integral scales of 0.40 (top) and 0.10 (bottom) of the flow domain.

Figure 4a Breakthrough curves from a 3-D porous medium for two realizations with the same $\sigma^2\lambda$'. One (marked by square) with λ' of 0.4 and σ of 2 and another (marked by triangles) with λ' of 0.1 and σ of 4.

Figure 4b Breakthrough curves from a 3-D porous medium for two realizations with the same $\sigma^2\lambda$'. One (marked by square) with λ' of 0.4 and σ of 1 and another (marked by triangles) with λ' of 0.1 and σ of 2.

Figure 5 Dispersivity (expressed as the inverse of Pe) as a function of the product $\sigma^2\lambda$ when 100 % of the tracer injected (top) and when only 50% of the tracer is recovered (bottom). Average values from 12 runs.

Figure 6. Ratio between T50 (arrival time for 50 % of the injected tracer) and Tmean (mean residence time) as a function of the product $\sigma^2\lambda$. Average values from 12 runs.

Figure 7. Experimental breakthrough curves for a) Amino G, b) iodide, and uranine. Results for 6 runs using a integral scale of 0.4 and corresponding standard deviation in hydraulic conductivity are also shown.

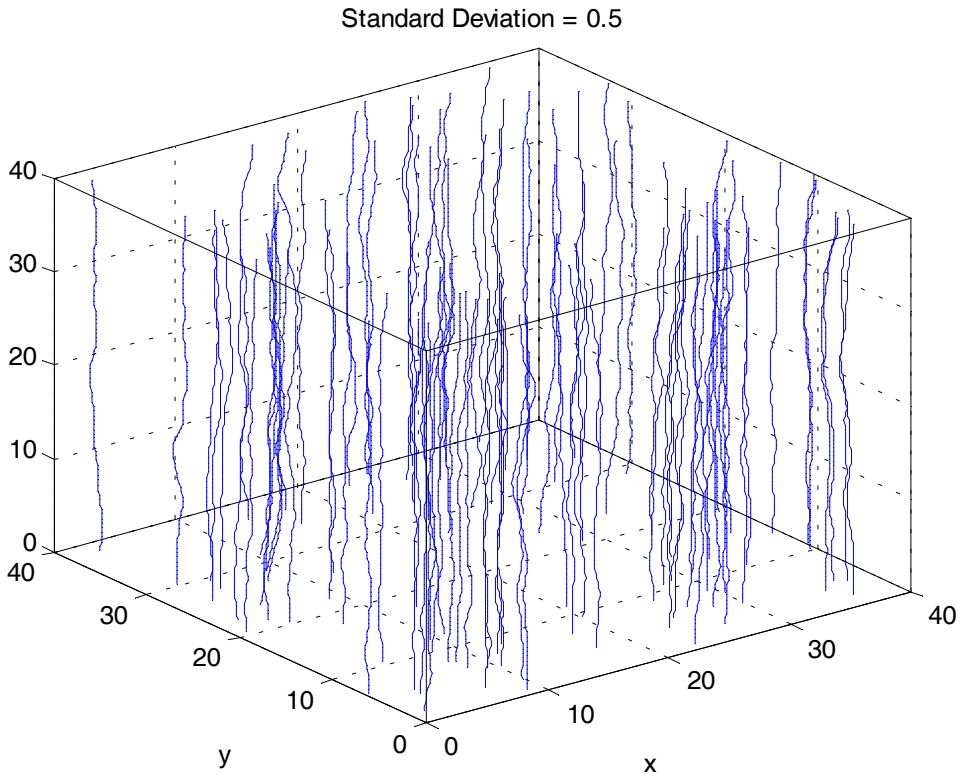
Standard Deviation = 0.5
40
30
20
10
0
40
30
20
10
0
y
0
10
20
30
40
x

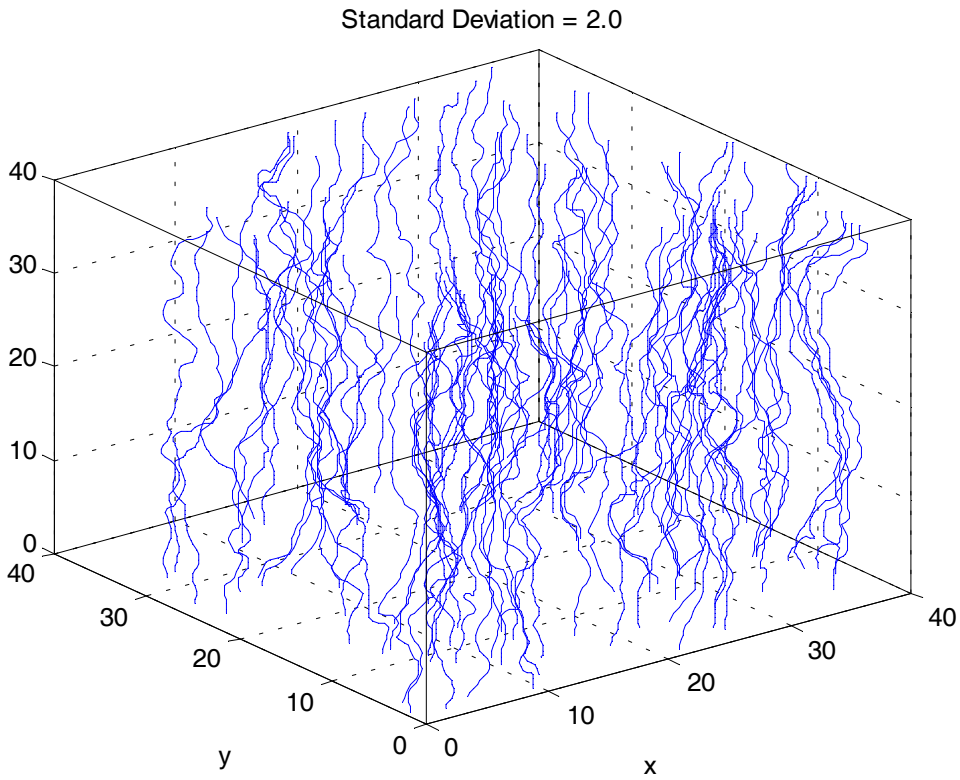
Standard Deviation = 2.0
40
30
20
10
0
40
30
20
10
0
y
0
10
20
30
40
x

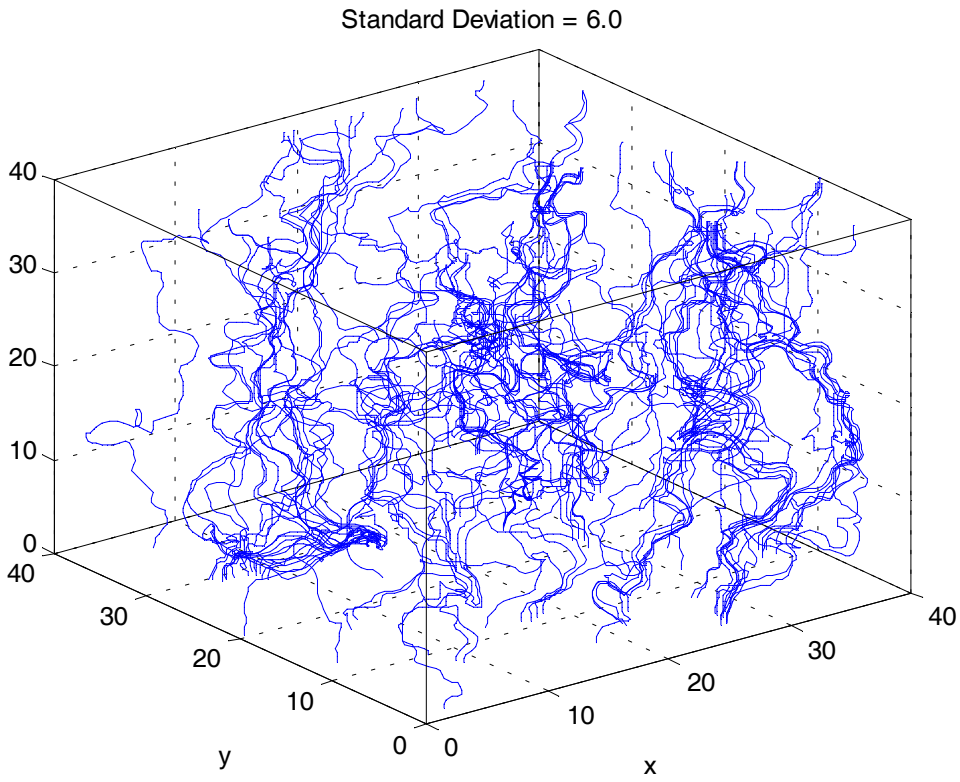

Figure 1. Emergence of channels for different standard deviation in hydraulic conductivity. A value of 0.20 is used for the integral range.

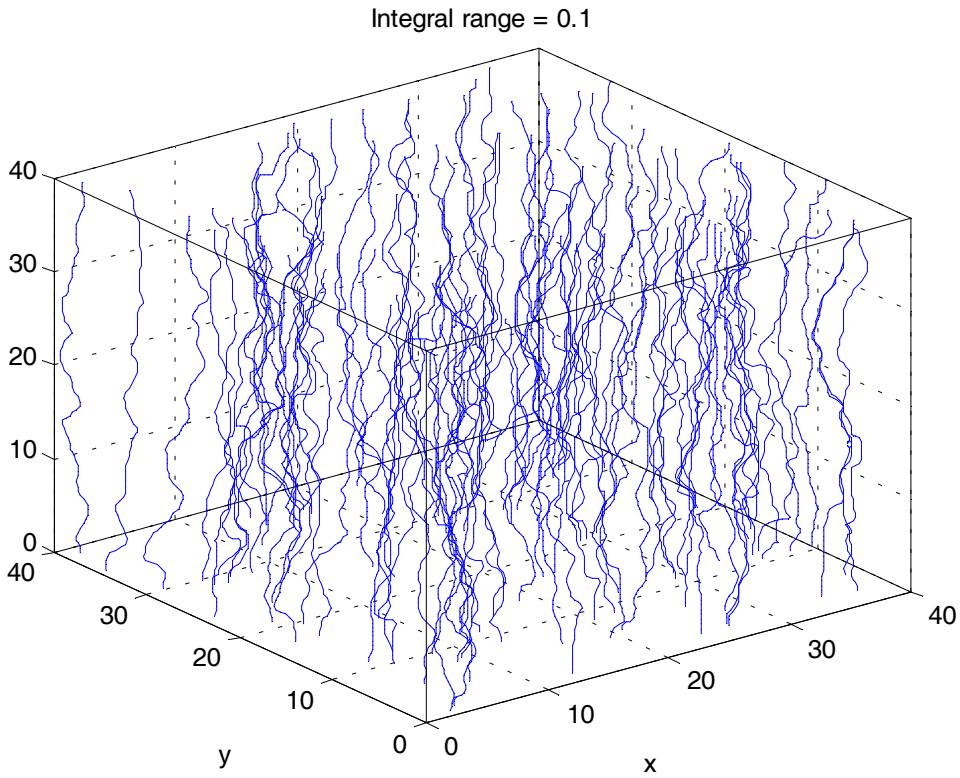
Integral range = 0.1
40
30
20
10
0
40
30
20
10
0
y
0
10
20
30
40
x

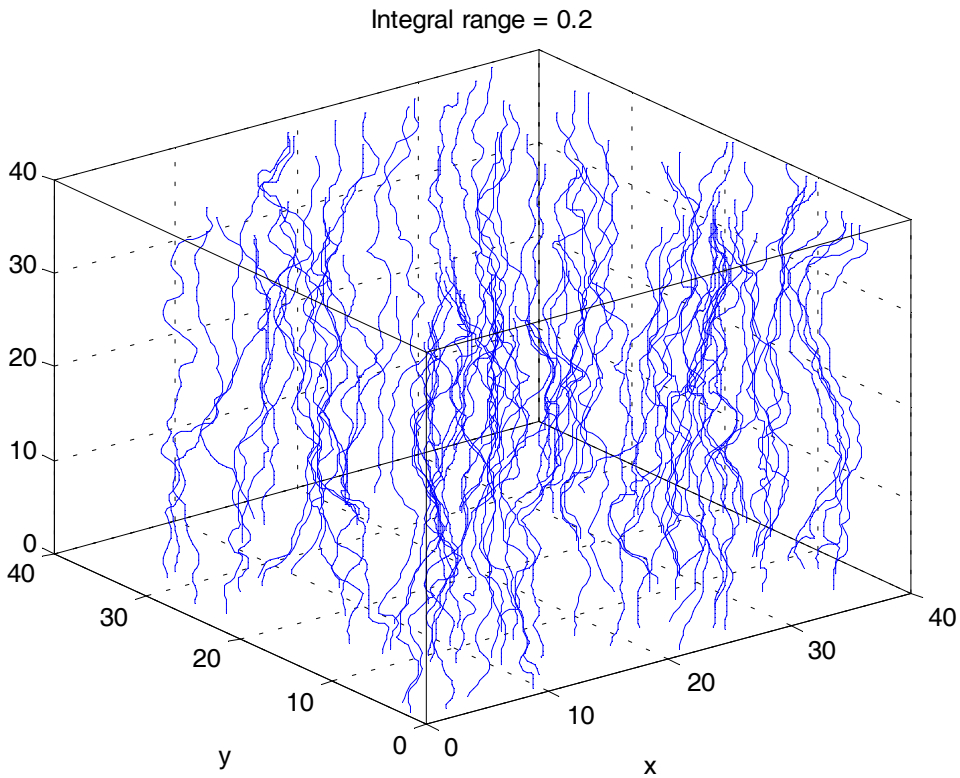
Integral range = 0.2
40
30
20
10
0
40
30
20
10
0
y
0
10
20
30
40
x

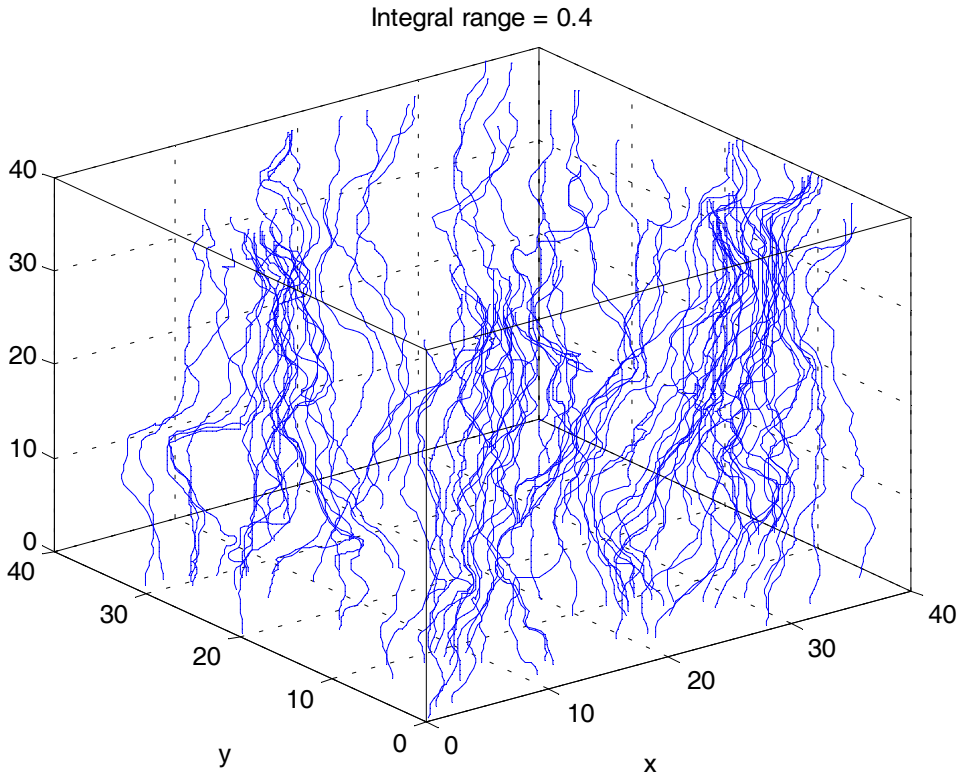

Figure 2. Emergence of channels for integral range. A value of 2.0 is used for the standard deviation of the conductivity distribution.

FIGURES Continuation

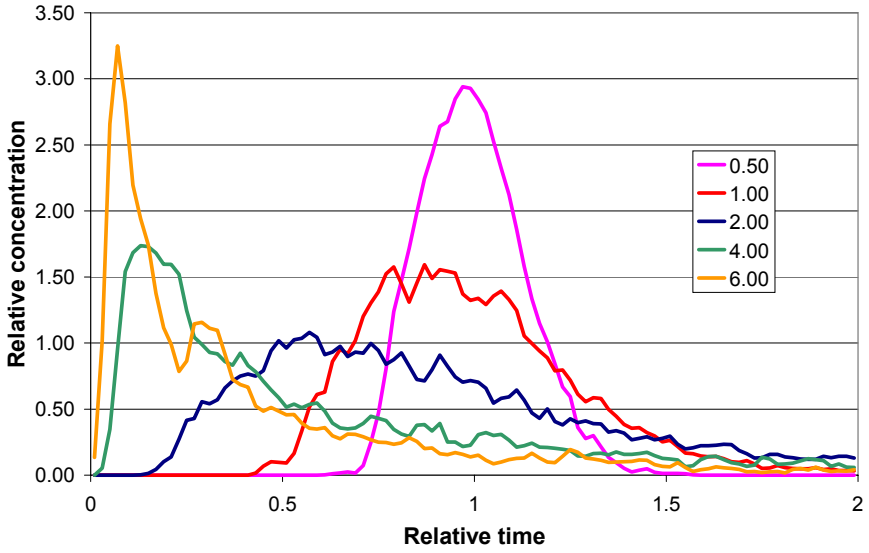

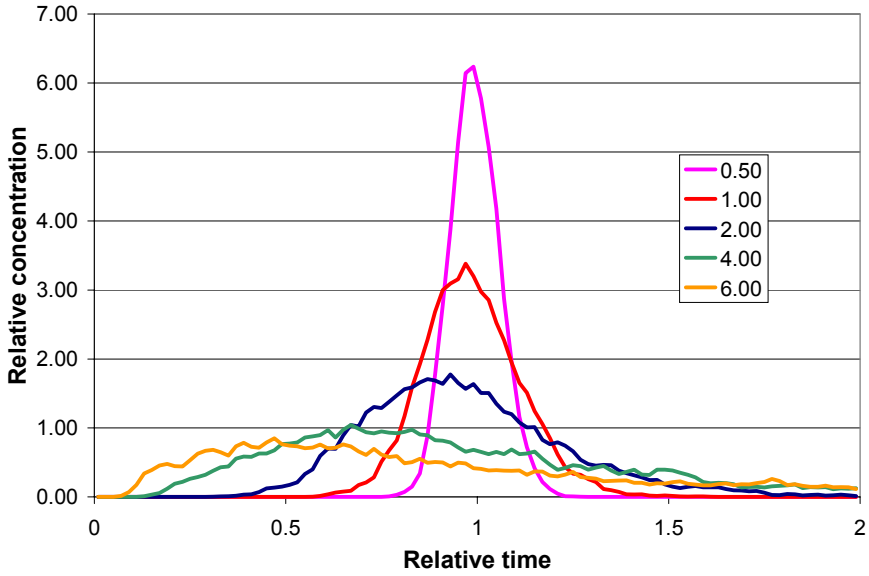

Figure 3 Breakthrough curves from a 3-D porous medium. For integral scales of 0.40 (top) and 0.10 (bottom) of the flow domain.

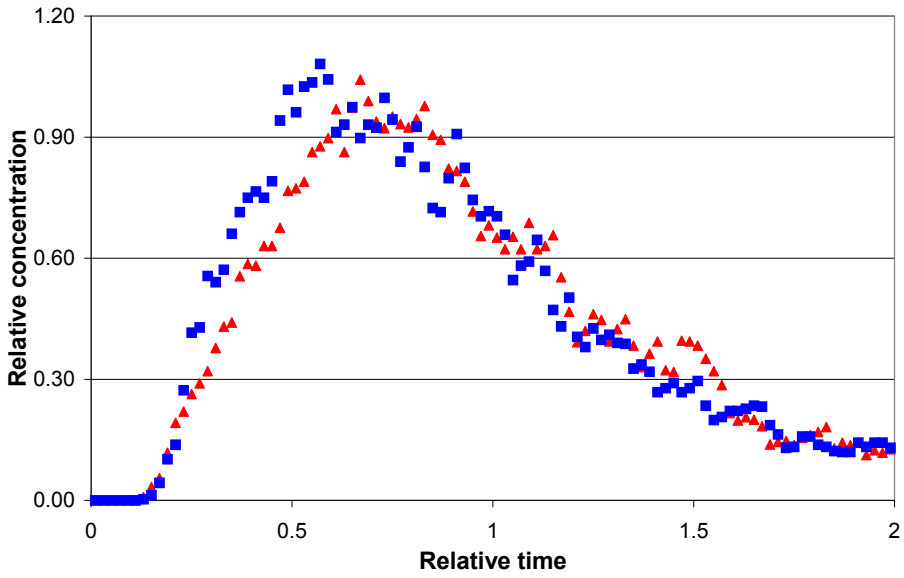

Figure 4a Breakthrough curves from a 3-D porous medium for two realizations with the same $\sigma^2\lambda'$. One (marked by square) with λ' of 0.4 and σ of 2 and another (marked by triangles) with λ' of 0.1 and σ of 4.

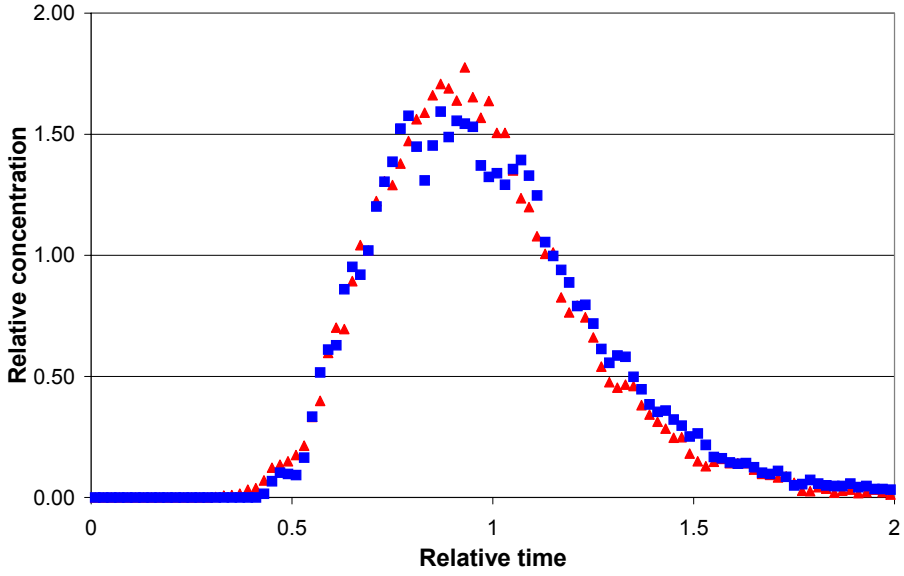

Figure 4b Breakthrough curves from a 3-D porous medium for two realizations with the same $\sigma^2\lambda'$. One (marked by square) with λ' of 0.4 and σ of 1 and another (marked by triangles) with λ' of 0.1 and σ of 2.

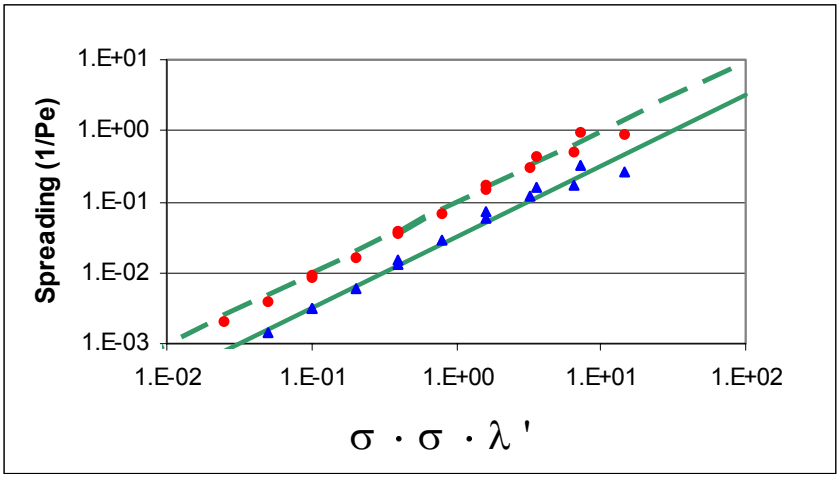

Figure 5 Dispersivity (expressed as the inverse of Pe) as a function of the product $\sigma^2\lambda$ when 100 % of the tracer injected (top) and when only 50% of the tracer is recovered (bottom). Average values from 12 runs.

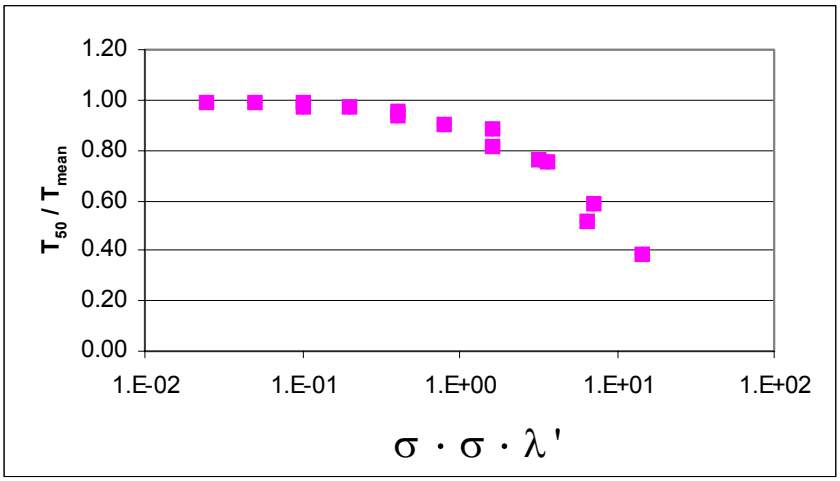

Figure 6. Ratio between T50 (arrival time for 50 % of the injected tracer) and Tmean (mean residence time) as a function of the product $\sigma^2\lambda$. Average values from 12 runs.

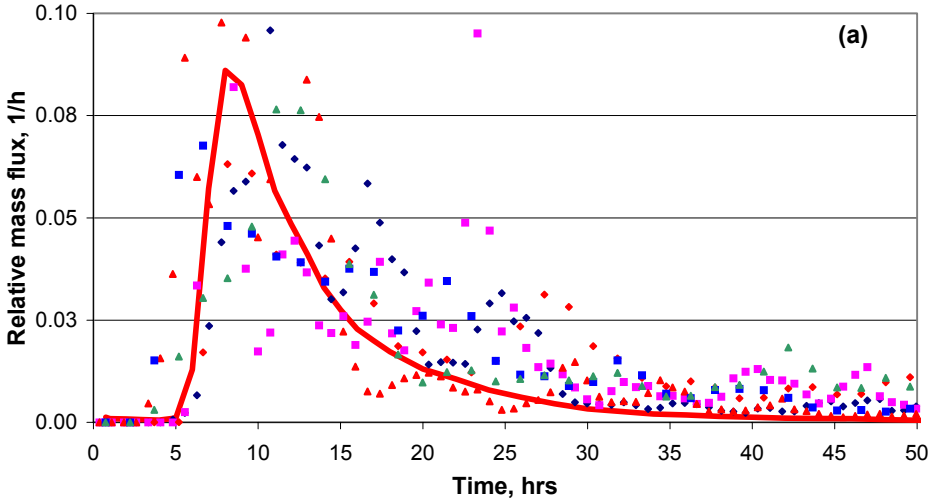
(a)
Relative mass flux, 1/h
0.10
0.08
0.05
0.03
0.00
0
5
10
15
20
25
30
35
40
45
50
Time, hrs

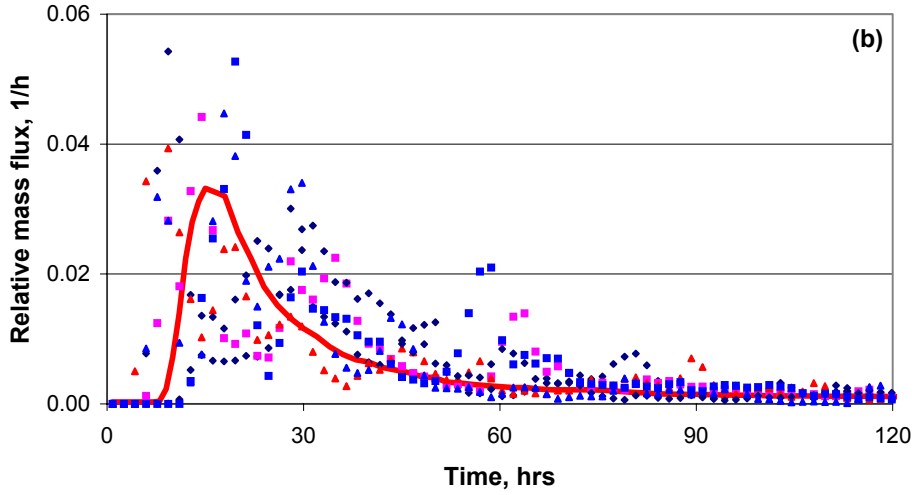
(b)
Relative mass flux, 1/h
0.06
0.04
0.02
0.00
0
30
60
90
120
Time, hrs

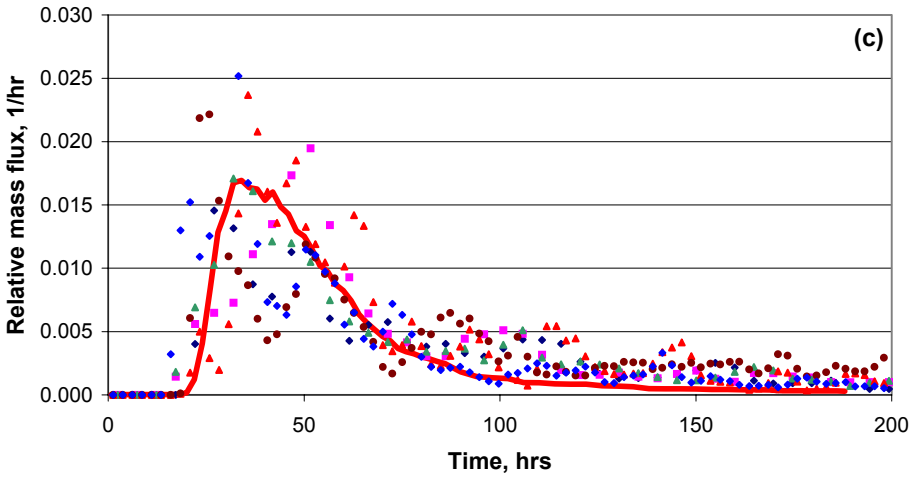

Figure 7. Experimental breakthrough curves for (a) Amino G, (b) iodide, and (c) uranine. Results for 6 runs using an integral scale of 0.4 and corresponding standard deviation in hydraulic conductivity are also shown.